

Reduced Order Model of a Neuron-Electrode Interface Coupled to a Hodgkin-Huxley Model

Ulrike Fitzer^{1,2}, Dennis Hohlfeld², Tamara Bechtold^{1,2}

¹Jade University of Applied Sciences

Friedrich-Paffrath-Straße 101, Wilhelmshaven, Germany

²Institute for Electronic Appliances and Circuits, University of Rostock

Albert-Einstein-Straße 2, Rostock, Germany

Ulrike.Fitzer@jade-hs.de

Dennis.Hohlfeld@uni-rostock.de

Tamara.Bechtold@jade-hs.de

Abstract – The electric properties of an interface between an electrode and a neuron are highly dependent on interface geometry and other parameters. Finite element models can be used to study these properties to a certain extent. Unfortunately, such models are computationally very expensive. By reducing these models, the computational time can be decreased. In this work, we use Krylov-subspace based model order reduction to reduce a simplified, linearized finite element model of an electrode-neuron interface. This facilitates the coupling to the Hodgkin-Huxley model at system level and reduces the computational time considerably. The accuracy of the original finite element model is preserved to a large extent.

Keywords: Neuron-Electrode Interface, Hodgkin-Huxley Model, Model Order Reduction, Finite Element Model

1. Introduction

Implantable neural interfaces are widely used in medical applications. They are also subject to research with different priorities, for example improving the medical treatment of patients or focusing on recording signals leading to a better understanding of the brain's function [1]. In all of these applications, the interface between electrodes and neurons has an important effect on the achieved result [2–4]. In vitro cultures of neuronal networks on microelectrode arrays can be used to study such effects [2, 4, 5].

Finite element models offer the possibility to simulate the interaction between electrodes and neurons. In [2], the authors investigated the electrical contact between a neuron placed on a planar substrate electrode using a finite element model. In [3, 6, 7], the Hodgkin-Huxley model [8] was combined with a similar finite element model. In [9], two modelling approaches are explained in detail: The hybrid approach, combining a finite element model of the electrical potential field with the calculation of the neuron's response using the cable equation, and a full finite element approach, allowing the simultaneous calculation of intracellular and extracellular potentials. The authors of [4] use a finite element model to examine the influence of neuronal morphology on the shape of extracellular recordings with microelectrode arrays.

Depending on the complexity of the model, computational times can be very long. Model order reduction (MOR) is an efficient tool to reduce computational times and memory requirements, while maintaining good accuracy of the original model. In general, the electrical behaviour of neurons is highly nonlinear and can be described by the Hodgkin-Huxley model [8]. Krylov-subspace based MOR can be used to replace the linear part of the electrical model by a surrogate of much smaller dimension, thereby reducing, the computational complexity of the entire system [10]. In this work, we use Krylov-subspace based model order reduction to reduce a finite element model of a neuron-electrode interface, which contains linear components of the Hodgkin-Huxley model. The remaining nonlinear features are subsequently connected to the reduced order model at system level.

Section 2 explains the setup of the entire model. The finite element model is introduced and the system level design of the complete model is described in detail. The Krylov-subspace based MOR methodology is explained in Section 3. Our simulation results are presented in Section 4. In Section 5 we summarize our findings and give an outlook to future work.

2. Case Study: Neuron-Electrode Interface

The Hodgkin-Huxley model describes the transmembrane current density as a sum of capacitive and ionic components [11]:

$$i_m = c_m \frac{dV_m}{dt} + (V_m - V_{Na})g_{Na}m^3h + (V_m - V_K)g_Kn^4 + (V_m - V_L)g_L \quad (1)$$

i_m is the transmembrane current per unit area, c_m is the membrane capacitance per area, and V_m is the membrane voltage. V_{Na} , V_K , V_L are the Nernst voltages for sodium, potassium, and leakage ions per area. The Nernst voltage describes the membrane potential at which the current flow due to electric forces cancels the diffusive flow, if the membrane was permeable to only this specific kind of ion [11, 12]. g_{Na} , g_K , g_L are the maximum sodium, potassium, and leakage conductance per area, and m , h , and n are gating variables, describing the opening state of the corresponding ion channel [4, 8, 11]. The gating variables are defined by differential equations according to [8], using a resting potential of $V_r = -65$ mV.

Our model consists of two parts. A finite element model of a cultured neuron placed on top of a planar electrode forms one part. The neuron and the surrounding culture medium are modelled as volume conductors. The membrane representation in the finite element model only describes a cross-membrane conductivity and a membrane capacitance. The other part, which describes the major part of the Hodgkin-Huxley membrane properties [8], is connected at system level and will be described in Section 2.2.

2.1. Finite Element Model

In our previous work [13], we adopted the finite element model of a cultured neuron and an electrode proposed in [2]. The finite element model presented here builds on the one presented in [13]. Our model, which is built using the software ANSYS version 2022 R1, is shown in Figure 1. A neuron is placed on top of a planar electrode and covers it completely. Only the soma (the cell body) of the neuron is modelled. The axon and dendrites are not represented. The neuron model has an elliptical profile with height $h_n = 5$ μm and radius $r_n = 7$ μm . It has a conductivity of $\sigma_n = 1.43$ S/m. Culture medium encloses the neuron with a conductivity of $\sigma_m = 1.65$ S/m. The electrode (radius $r_e = 5$ μm) is placed at the bottom of the lower culture medium. It is represented by a surface body. Its finite element nodes are coupled at the same electric potential. Electro-chemical effects, which can occur at the interface between the electrode and the culture medium, are not considered in our model. A narrow sealing gap of 10 nm thickness between substrate and neuron, filled with culture medium, is implemented with a thickness of 0.5 μm . Its material parameters are adjusted proportionally as proposed in [2].

The neuronal membrane is not represented by a voluminous body. Only the portion of the membrane, which is modelled as part of the finite element model, is described in this Section. As shown in Figure 2, the membrane is divided into an upper and a lower part. The nodes of the respective surfaces are coupled in the voltage domain. The lower membrane above the electrode and the upper membrane are each modelled using one lumped resistor, representing the leakage resistance, and a lumped capacitor, representing the membrane capacitance. The leakage conductivity per area of the membrane is $G_L = 0.3$ mS/cm², and the capacitance per area is $c_{mem} = 0.1$ $\mu\text{F}/\text{cm}^2$ [14].

The sealing gap is divided into three rings (only one node of the middle ring is shown in Figure 2). The nodes of each ring are also coupled in the voltage domain. Each ring is connected to the neuron with one resistor and one capacitor in parallel, each component having the conductivity or the capacitance according to the area it represents. This is possible, because we only consider the concentric scenario where the neuron covers the electrode completely. In a more general case, where the neuron is placed off-center, our approach is not applicable as the potential varies with angular and radial coordinates. Also, a more detailed representation of the neuron including dendrites and axon is not possible with this approach.

A boundary condition of 0 V is imposed on the surface of the outer domain boundary of the culture medium and the sealing gap. This represents a counter electrode, which is far away from the neuron-electrode interface. Exploiting symmetry, the finite element model represents only one half of the interface. The other half is accounted for by a symmetry boundary condition.

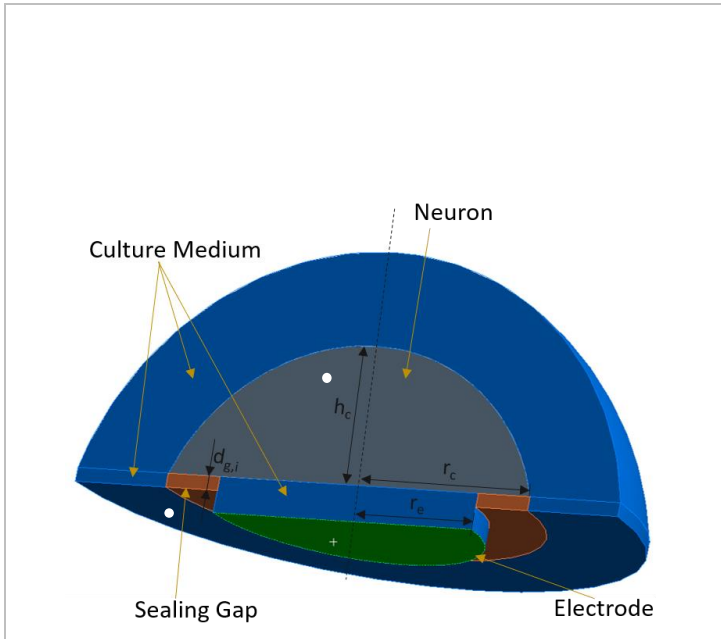


Figure 1: Model of our simplified neuron-electrode interface, based on [2]. A neuron is placed on a planar substrate electrode. The substrate is not part of the finite element model. Culture medium surrounds the neuron. A narrow sealing gap of 10 nm thickness between substrate and neuron is implemented with a thickness of 0.5 μm . Its material parameters are adjusted accordingly. The white marks show the points used for comparison of the electric potential between the full order model and the reduced order model.

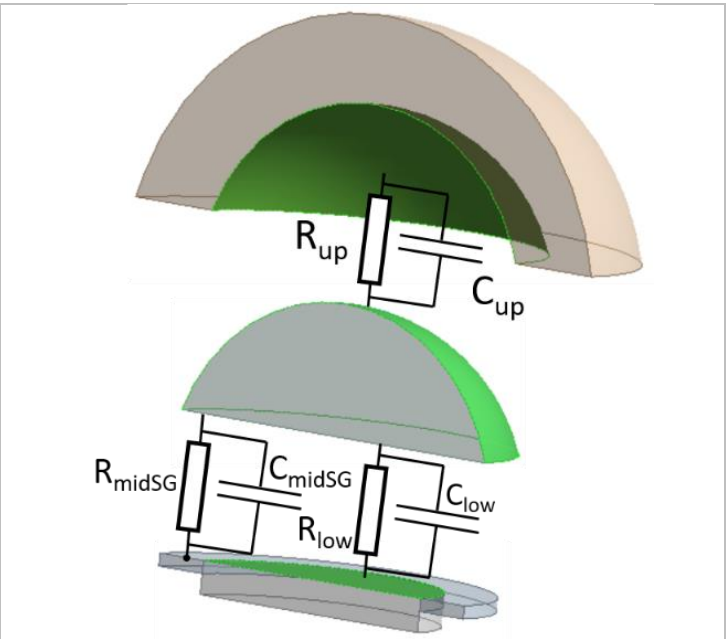


Figure 2: For the membrane representation in the finite element model, the voltage degrees of freedom have been coupled at the surfaces of the culture medium which touch the neuron, at the upper, and at the lower surface of the neuron. A lumped resistor and a lumped capacitor are inserted, which represent the leakage resistance and the membrane capacitance of the top and bottom part of the membrane. The contact between the sealing gap and the neuron is modelled in a similar manner. The sealing gap is divided into three rings (for clarity, only one node of the middle ring is shown here). Each ring is coupled in the voltage domain and connected to the lower surface of the neuron with a resistor and a capacitor in parallel.

2.2. System Level Model

After reduction of the finite element model, the reduced order model is transformed into a system-level representation. As such, it can be co-simulated with electrical circuits, that is, connected to realistic current sources, filters, amplifiers, and other electrical components [13]. The system level representation is created using the VHDL-AMS standard [15] and then imported into Ansys Twin Builder version 2022 R1. It has one input pin called 'elec', where the stimulus current can be applied to the electrode. Furthermore, four pins, each representing one of the surfaces of the membrane, allow the connection of the respective membrane nodes via a circuit, simulating Hodgkin-Huxley dynamics (see Figure 3).

The Potassium and Sodium branches are completely modelled at system level. Since the voltage source of the leakage branch is not included in the reduced order model, it has to be represented at system level, too. This was achieved by connecting an equivalent current source (I_L) in parallel [16]. A voltmeter measuring the transmembrane voltage delivers the necessary data to calculate the transfer rate coefficients. The ionic conductance is calculated in a separate system of equation blocks.

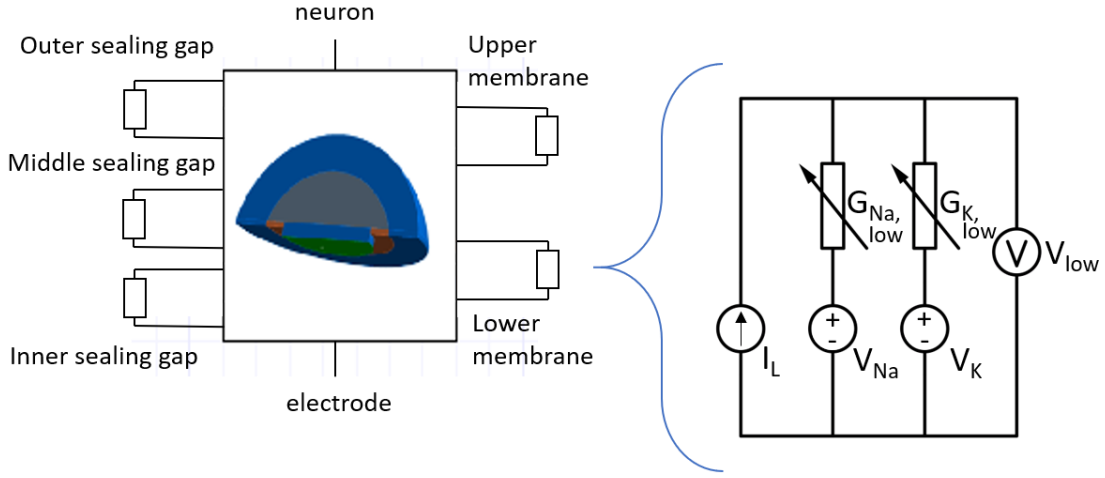


Figure 3: System level model of the reduced order model with its six pins. A current source can be connected to the electrode. The remaining circuit elements necessary to model the Hodgkin-Huxley dynamics [8], which are not included in the finite element model, can be connected between nodes representing the upper and lower membrane, and the membrane at the sealing gap.

3. Model Order Reduction

The process of model order reduction follows the method described in [13]. The partial differential equation for electric scalar potential can be written as:

$$-\nabla \cdot ([\sigma] \nabla V) - \nabla \cdot \left([\varepsilon] \nabla \frac{\partial V}{\partial t} \right) = 0 \quad (2)$$

where $[\sigma]$ is the electrical conductivity matrix, $[\varepsilon]$ is the permittivity matrix, V is the scalar electric potential, and t is the time. The numerical analysis of the simplified neuron-electrode interface is carried out by finite element method. After spacial discretization, Equation 2 can be represented as a system of n ordinary differential equations:

$$\sum_n \begin{cases} C\dot{x}(t) + Gx(t) = Bu(t) \\ y(t) = E^T x(t) \end{cases} \quad (3)$$

with state vector $x(t) \in R^n$, input vector $u(t) \in R^m$, output vector $y(t) \in R^p$, permittivity matrix $C \in R^{n \times n}$, electrical conductivity matrix $G \in R^{n \times n}$, input distribution matrix $B \in R^{n \times m}$, and output matrix $E \in R^{n \times p}$.

Krylov based MOR [10] approximates Equation 3 by a system of the same form, but with much smaller order r :

$$\sum_n \begin{cases} C_r \dot{z}(t) + G_r z(t) = B_r u(t) \\ y(t) = E_r^T z(t) \end{cases} \quad (4)$$

where $z \in R^r$ is the state vector of the reduced order model. Further, permittivity matrix and electrical conductivity matrix $C_r, G_r \in R^{r \times r}$, input distribution matrix $B_r \in R^{r \times m}$, output matrix $E_r \in R^{r \times p}$, and $r \ll n$. Equation 4 is gained by an orthonormal projection of Equation 3 onto the right Krylov-subspace, defined as:

$$K_r^R = \text{span}\{r, Ar, A^2r, \dots, A^{r-1}r\} \quad (5)$$

with $A = -G^{-1}C$ and $r = -G^{-1}B$. It holds $C_r = V^T C V$, $G_r = V^T G V$, $B_r = V^T B$, and $E_r = V^T E$, where V is an orthonormal basis of Equation 4 $\text{colspan}\{V\} = K_r^R$, which is created by the Block Arnoldi algorithm [10]. An inherent property of the Krylov subspace is, that the transfer functions $H(s)$ and $H_r(s)$ of Equations 3 and 4 respectively, when expanded into a Taylor series around some point s_0 :

$$H(s) = E^T (G + sC)^{-1} B = \sum_0^{\infty} m_i (s - s_0)^{-1} \quad (6)$$

$$H_r(s) = E_r^T (G_r + sC_r)^{-1} B_r = \sum_0^{\infty} m_{r,i} (s - s_0)^{-1} \quad (7)$$

match in the first r coefficients: $m_i = m_{r,i}, i = 0, \dots, r$. These coefficients are called moments or Markov parameters (depending on the chosen expansion point) and are defined as $m_i = (-1)^i E^T (G^{-1}C)^i G^{-1} B$ for $i = 0, 1, 2, \dots$

We deploy the implementation within “Model reduction inside Ansys” [17].

4. Numerical Simulation Results

We first create the linear finite element model in Ansys. Then, this model is reduced and compared to the original full-size model. Finally, it is coupled to the nonlinear part of the Hodgkin-Huxley model at system level.

All simulations are carried out using an Intel Xenon Processor (Skylake, IBRS) with 2.99 GHz (2 Processors with 6 cores each). A 0.5 nA stimulus current is applied to the electrode during a transient simulation. The full order model (FOM) has 8245 degrees of freedom and the reduced order model (ROM) has 30 degrees of freedom. It takes approximately 0.35 seconds to construct the reduced order model. After construction, the ROM can be used for multiple simulations without having to create it again. While it takes 69 seconds to calculate transient solution of the FOM, it only takes 2.2 seconds to calculate the ROM (see Table 1). The computational time is therefore reduced to 3.2% of the time necessary to calculate the FOM.

Table 1: CPU time comparison between FOM and ROM Intel Xenon Processor (Skylake, IBRS) with 2.99 GHz (2 Processors with 6 cores each)

	FOM	ROM
Number of DOFs	8245	30
Computational time [s]	69	2.2

Figures 4 and 5 show the comparison between the potential development over time. Here, an expansion point of $s_0 = 0$ is used. The reduced order model matches the full order model very well. At the electrode, a maximum relative error of only 4.7×10^{-11} percent is observed. The relative error inside the neuron increases throughout the simulation to a maximum of 1.6×10^{-10} percent. By altering the expansion point, the error can be influenced at different simulation times. Figure 6 shows the relative error of the reduced order model at both points using an expansion point of $s_0 = 10^7$.

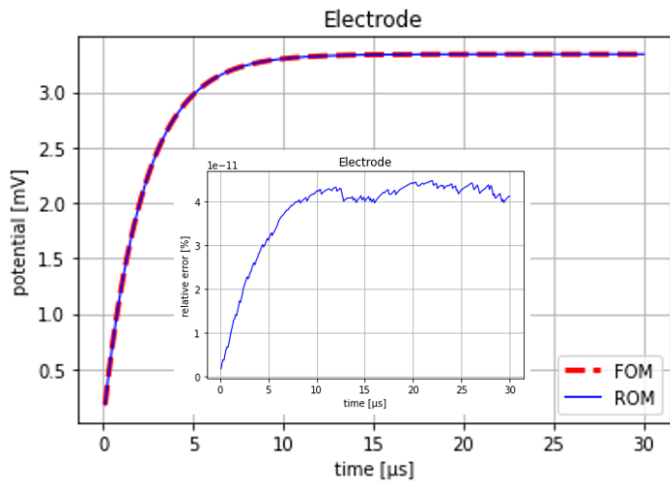


Figure 4: Development of the electric potential at the node representing the electrode when applying a 0.5 nA stimulus current to the electrode. The ROM matches the FOM very well with a maximum error of only 4.7×10^{-11} percent.

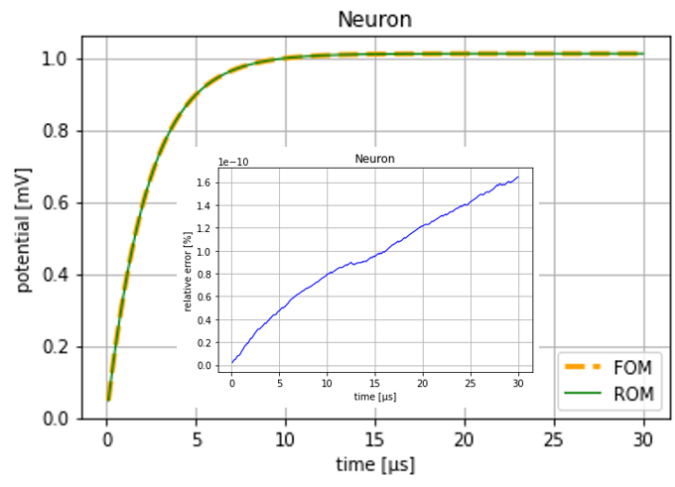


Figure 5: Development of the electric potential at the node inside the neuron. The error is increasing throughout the simulation to 1.6×10^{-10} percent.

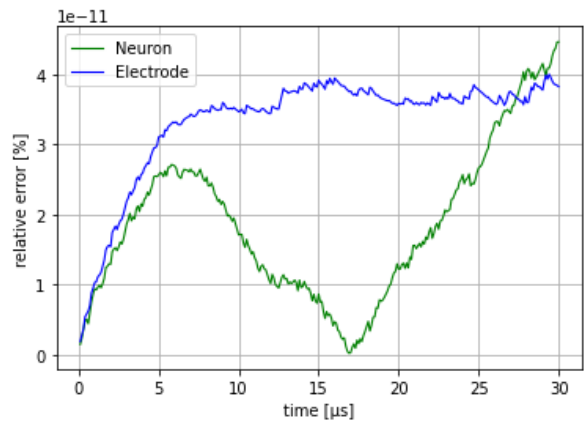


Figure 6: Error of the reduced order model at the electrode and inside the neuron. The reduced order model is created with an expansion point of $s_0 = 10^7$.

At system level, the remaining circuit elements for the Hodgkin-Huxley representation are connected according to Section 2.2. We connected an ideal current source to the electrode and conducted a transient simulation for 90 ms with a stepsize of 0.04 ms. The electrode is stimulated with -5 nA between 40 seconds and 60 seconds of simulation time. The voltage development at the membrane and at the electrode is shown in Figure 7. The initial condition for the simulation is a potential of 0 volt in the entire domain. This leads to a long stabilization process for the first 32 ms, before the resting potential of -65 mV is reached. An action potential is created like in [3] (however, the authors of [3] used a different geometry and different stimulation parameters). The simulation took 8.66 seconds.

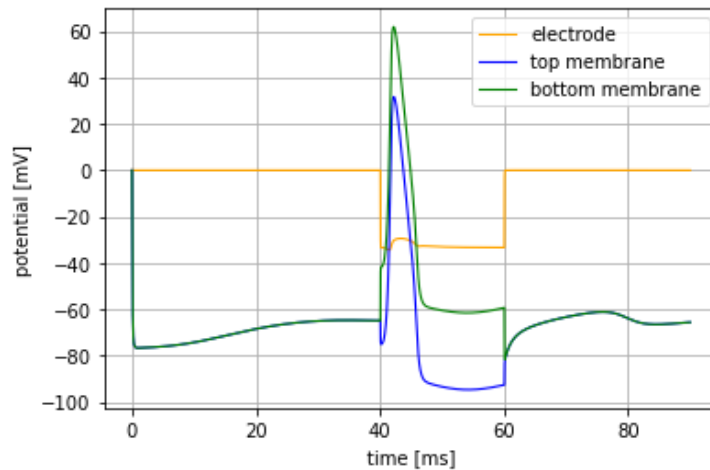


Figure 7: Hodgkin-Huxley membrane properties are combined with the reduced order model on system level. The electrode is stimulated with -5 nA between 40 seconds and 60 seconds of a transient simulation. In the beginning, an initial condition of 0 volt in the whole domain leads to a long stabilization process until a resting potential of -65 mV is reached. During stimulation, an action potential is created. The complete simulation took 8.66 seconds.

5. Conclusion and Outlook

In this work we used Krylov-subspace based model order reduction to reduce computational complexity of a linear finite element model of a neuron-electrode interface. We then connected the remaining nonlinear elements of the Hodgkin-Huxley membrane representation to the system level version of the reduced order model. We were able to significantly reduce the computational time for the finite element model while keeping the error of the reduced order model very small.

However, the method presented here does not hold for the general case. By coupling nodes of surfaces with similar potential in the voltage domain, we kept the number of Hodgkin-Huxley circuits, which had to be added on system level, small. Clearly, this method only works with our symmetric geometry. Moving the neuron off-center or changing the elliptical profile of the neuron to a more detailed geometry including axon or dendrites will make it impossible to couple the nodes in the different parts of the membrane.

In the future, it is therefore necessary to include the complete Hodgkin-Huxley dynamics in the finite element model, which will make it nonlinear. We plan to develop and employ suitable methods of model order reduction. A promising approach is MOR via artificial neural networks [18].

References

- [1] C. Boehler, S. Carli, L. Fadiga, T. Stieglitz, and M. Asplund, "Tutorial: guidelines for standardized performance tests for electrodes intended for neural interfaces and bioelectronics," *Nature protocols*, vol. 15, no. 11, pp. 3557–3578, 2020, doi: 10.1038/s41596-020-0389-2.
- [2] J. R. Buitengeweg, W. L. Rutten, and E. Marani, "Finite element modeling of the neuron-electrode interface," *IEEE Eng. Med. Biol. Mag.*, vol. 19, no. 6, pp. 46–52, 2000, doi: 10.1109/51.887245.
- [3] J. R. Buitengeweg, W. Rutten, and E. Marani, "Geometry based dynamic modeling of the neuron-electrode interface," in *Proceedings of the 22nd Annual International Conference of the IEEE Engineering in Medicine and Biology Society (Cat. No.00CH37143)*, Chicago, IL, USA, 2000, pp. 2004–2007.
- [4] R. Bestel, U. van Rienen, C. Thielemann, and R. Appali, "Influence of Neuronal Morphology on the Shape of Extracellular Recordings With Microelectrode Arrays: A Finite Element Analysis," *IEEE transactions on bio-medical engineering*, vol. 68, no. 4, pp. 1317–1329, 2021, doi: 10.1109/TBME.2020.3026635.

- [5] R. Bestel, R. Appali, U. van Rienen, and C. Thielemann, “Effect of Morphologic Features of Neurons on the Extracellular Electric Potential: A Simulation Study Using Cable Theory and Electro-Quasi-Static Equations,” *Neural computation*, vol. 29, no. 11, pp. 2955–2978, 2017, doi: 10.1162/neco_a_01019.
- [6] J. R. Buitengeweg, W. L. C. Rutten, and E. Marani, “Geometry-based finite-element modeling of the electrical contact between a cultured neuron and a microelectrode,” *IEEE transactions on bio-medical engineering*, vol. 50, no. 4, pp. 501–509, 2003, doi: 10.1109/TBME.2003.809486.
- [7] W. Rutten *et al.*, “Neuroelectronic interfacing with cultured multielectrode arrays toward a cultured probe,” *Proc. IEEE*, vol. 89, no. 7, pp. 1013–1029, 2001, doi: 10.1109/5.939810.
- [8] A. L. HODGKIN and A. F. HUXLEY, “A quantitative description of membrane current and its application to conduction and excitation in nerve,” *The Journal of physiology*, vol. 117, no. 4, pp. 500–544, 1952, doi: 10.1113/jphysiol.1952.sp004764.
- [9] S. Joucla, A. Glière, and B. Yvert, “Current approaches to model extracellular electrical neural microstimulation,” *Frontiers in computational neuroscience*, vol. 8, p. 13, 2014, doi: 10.3389/fncom.2014.00013.
- [10] R. W. Freund, “Krylov-subspace methods for reduced-order modeling in circuit simulation,” *Journal of Computational and Applied Mathematics*, vol. 123, 1-2, pp. 395–421, 2000, doi: 10.1016/S0377-0427(00)00396-4.
- [11] J. Malmivuo and R. Plonsey, *Bioelectromagnetism - Principles and Applications of Bioelectric and Biomagnetic Fields*: Oxford University Press, 1995.
- [12] P. Dayan and L. F. Abbott, *Theoretical neuroscience: Computational and mathematical modeling of neural systems*. Cambridge, Mass.: MIT Press, 2001. [Online]. Available: <http://site.ebrary.com/lib/librarytitles/docDetail.action?docID=10229582>
- [13] Ulrike Fitzer, Dennis Hohlfeld, Tamara Bechtold, “Reduced Order Modelling of a Neuron-Electrode Interface,” in *Proc. 23rd International Conference on Thermal, Mechanical, and Multi-Physics Simulation and Experiments in Microelectronics and Microsystems (EuroSimE)*, 2022.
- [14] C. T. M. Choi and S.-J. You, “Finite Element Models of Neuron Electrode Sealing Interfaces,” *IEEE Trans. Magn.*, vol. 48, no. 2, pp. 643–646, 2012, doi: 10.1109/TMAG.2011.2175717.
- [15] *IEEE Standard VHDL Analog and Mixed-Signal Extensions*, Piscataway, NJ, USA.
- [16] D. H. Johnson, “Scanning our past origins of the equivalent circuit concept: the current-source equivalent,” *Proc. IEEE*, vol. 91, no. 5, pp. 817–821, 2003, doi: 10.1109/JPROC.2003.811795.
- [17] E. B. Rudnyi, “MOR for ANSYS,” in *Advanced Micro and Nanosystems*, vol. 10, *System-level modeling of MEMS*, T. Bechtold, G. Schrag, and L. Feng, Eds., Weinheim: Wiley-VCH-Verl., 2013, pp. 425–438.
- [18] Q. Zhuang, J. M. Lorenzi, H.-J. Bungartz, and D. Hartmann, “Model order reduction based on Runge–Kutta neural networks,” *DCE*, vol. 2, 2021, doi: 10.1017/dce.2021.15.